sustainability

MDPI

Article

The Relationship between Residential Block Forms and Building Carbon Emissions to Achieve Carbon Neutrality Goals: A Case Study of Wuhan, China

Haitao Lian [1,2], Junhan Zhang [3], Gaomei Li [4,5,*] and Rui Ren [1,6]

1 School of Architecture, Tianjin University, Tianjin 300072, China; lianhaitao@hebeu.edu.cn (H.L.); rui.ren@polimi.it (R.R.)
2 School of Architecture and Design, Hebei University of Engineering, Handan 056038, China
3 Stuart Weitzman School of Design, University of Pennsylvania, Philadelphia, PA 19104, USA; apply_zjunhan2023@163.com
4 School of Architecture & Urban Planning, Huazhong University of Science and Technology, Wuhan 430030, China
5 Hubei Engineering and Technology Research Center of Urbanization, Wuhan 430074, China
6 Department of Architecture and Urban Studies, Politecnico di Milano, 20158 Milan, Italy
* Correspondence: li_gm@hust.edu.cn; Tel.: +86-13381390393

Abstract: Controlling building carbon emissions (CEs) is key to achieving the goal of carbon neutrality. Residential blocks are the main contributors of buildings' carbon emissions and intensity, and thus can be manipulated to achieve carbon neutrality. This work aimed to evaluate the building carbon emissions intensity (CEI) levels of residential blocks using Rhino and Grasshopper and to quantify the relationship between the block form parameters and a building's carbon emissions (CEs). Firstly, 48 cases were selected by stratified sampling, and they were classified by architectural typology. Secondly, the residential block morphological parameters and building carbon emissions were calculated. Thirdly, the relationship between the block form parameters and the building's CE was quantified using statistical methods. Lastly, low-carbon planning strategies for residential blocks under the target of carbon neutrality were proposed. The findings showed that the influence of the block form parameters on a building's CE was 31.66%. A building's shape factor has a positive influence on its CE, and the floor area ratio, building volume–site area ratio, and building height have negative influences on its CE. A building's shape factor, cover ratio, and surface–site area ratio synergistically impact its CE. The weight of a building's shape factor on its carbon emissions was 3.84 times that of its cover ratio and 4.46 times that of its surface–site area ratio. The technology workflow proposed in this study can provide data in support of carbon emissions assessments and low-carbon planning strategies for urban blocks in other cities in China and worldwide.

Keywords: carbon neutral; residential blocks; block form; building carbon emissions; low-carbon planning

Citation: Lian, H.; Zhang, J.; Li, G.; Ren, R. The Relationship between Residential Block Forms and Building Carbon Emissions to Achieve Carbon Neutrality Goals: A Case Study of Wuhan, China. *Sustainability* **2023**, *15*, 15751. https://doi.org/10.3390/su152215751

Academic Editors: Jiaqiang Wang, Linfeng Zhang and Sungmin Yoon

Received: 14 September 2023
Revised: 1 November 2023
Accepted: 2 November 2023
Published: 8 November 2023

1. Introduction

1.1. Background

Cities consume a significant amount of fossil energy globally and are responsible for over 70% of global greenhouse gas emissions [1]. Urban energy consumption makes up approximately two-thirds of the total global energy consumption [2]. The primary sectors contributing to urban energy consumption are industry, transportation, and buildings [3]. Specifically, building energy consumption (BEC) constitutes 60% of the combined energy consumption from these sectors [2]. As reported by the International Energy Agency (IEA), in 2021, the building operation and building construction sectors consumed 30% of the energy produced, and they produced approximately 15% of the direct CO_2 emissions. In 2018, the building energy consumption (BEC) and carbon emissions (CEs) of China were

examined, revealing that BEC during the operational stage accounted for 21.7% of the total national energy consumption. The construction area was measured at 67.1 billion m^2, and the CE reached 2.1 billion CO_2. Residential buildings represented the largest proportion in terms of the BEC, CE, and total building area. Notably, urban residential buildings accounted for 42% of the CE [4]. Thus, controlling residential buildings' CEs is the inevitable choice for achieving two carbon goals: striving toward peak CO_2 emissions by 2030 and endeavoring to achieve carbon neutrality by 2060 for sustainable development in our country.

In September 2020, during the 75th General Debate of the United Nations General Assembly, President Xi Jinping articulated that the Paris Agreement for combating climate change represented the general direction of a global green and low-carbon transition, that it is the fundamental action needed to protect the Earth as our homeland, and that all countries must take resolute steps forward. Concurrently, he declared that China would increase its nationally determined contribution, adopt robust policies and measures, strive toward peak CO_2 emissions by 2030, and endeavor to achieve carbon neutrality by 2060 [5].

As the world's largest developing country, China has introduced many policies and measures to achieve its dual carbon goals: a carbon peak by 2030 and carbon neutrality by 2060 through the following:

(1) Building a green, low-carbon, and circular economic system for the new era: China has made systematic developments for a green, low-carbon, and circular economic system, promoting comprehensive coverage in the areas of production, distribution, and consumption, accelerating the greening of agriculture and industry, developing green industries, and building green supply chains.
(2) Enhancing energy-use efficiency: Optimizing and adjusting China's industrial structure are its fundamental approach to improve its energy-use efficiency, strengthen the refined management of enterprises, accelerate the construction of a modern industrial system, and obtain the highest economic and social benefits while minimizing the toll on resources and the environment, which will result in an all-around improvement in the efficiency of resource use.
(3) Increasing the proportion of non-fossil energy consumption: In order to reduce its proportion of fossil energy consumption, China has begun to vigorously develop new types of energy, increase the proportion of renewable energy it uses, promote the development of wind power and photovoltaic power generation, and develop hydroelectric energy, geothermal energy, ocean energy, hydrogen energy, biomass energy, and photothermal power generation tailored to regional conditions.
(4) Reducing its levels of carbon dioxide emissions: China is currently accelerating the promotion of a comprehensive green transformation of industrial development, integrating the requirements of the carbon peak and carbon neutrality targets into the entire process of economic and social development and within all areas. It is vigorously promoting energy conservation and emissions reduction, comprehensively implementing cleaner production, accelerating the development of the recycling economy, strengthening the comprehensive use of resources, and continuously upgrading its levels of green, low-carbon, and recycling development.
(5) Enhancing the carbon sink capacity of ecosystems: For China to achieve its goals for the carbon peak and carbon neutrality on schedule, an important aspect will be to enhance the capacity of ecological carbon sinks, strengthen land use spatial planning and use regulation, and effectively bring into play the carbon sequestration functions of forests, grasslands, wetlands, oceans, soils, and permafrost so as to enhance the incremental amounts of ecosystem carbon sinks [6].

1.2. Literature Review

1.2.1. Building Carbon Emissions (CEs) Assessments

China's initial step towards achieving its dual carbon goals involved evaluating its CEs. Given the significant role the building sector plays in these emissions, researchers

have directed their attention to this area. The assessment models for building CEs can be categorized as either top-down or bottom-up approaches [7].

The top-down approach involves estimating the overall building carbon emissions before carrying out down-scaling analyses in time and space, and the bottom-up approach involves calculating the hour-by-hour energy consumption of individual buildings before scaling up to the regional level for carbon emissions calculations. Kavgic et al. [8] made a comparative analysis of the ideas of the two evaluation methods, as shown in Figure 1. Yang et al. [9] established a method for measuring carbon emissions from urban buildings based on the theory of a building's life cycle, and they used the STIRPAT model to analyze the factors affecting carbon emissions from buildings in Beijing. This model uses the top-down approach. The study's findings indicated that the most significant factor that influenced carbon emissions from buildings in Beijing was population urbanization, followed by the per capita building living area and the per capita disposable income, while the total population had a relatively small effect.

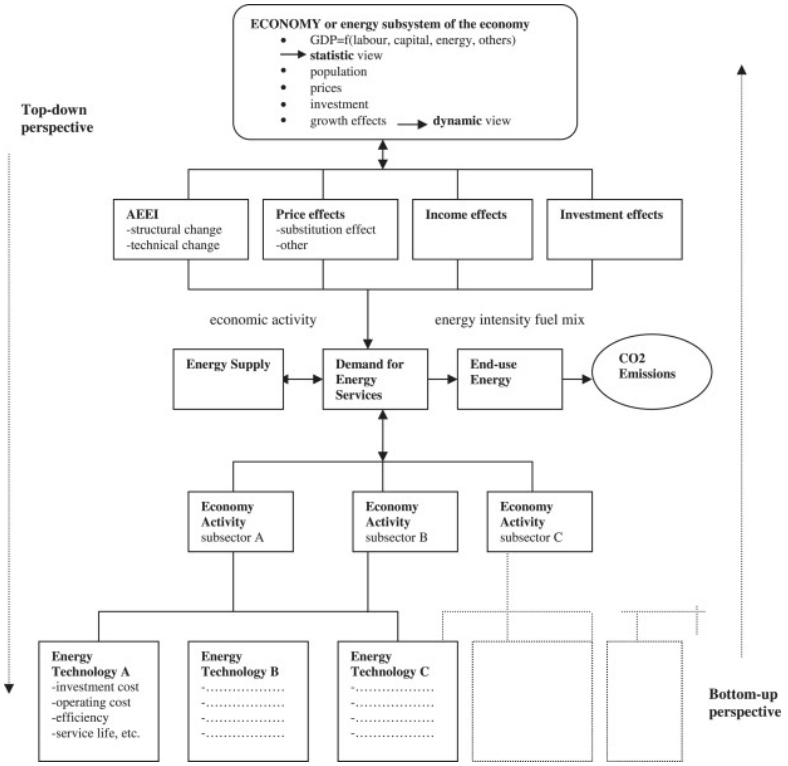

Figure 1. A comparative analysis of the ideas of the two evaluation methods [8].

In order to explore the control path of China's total building carbon emissions, Yang et al. [10] established the China Building Carbon Emission Model (CBCEM) from China's overall emissions reduction target, which adopted a bottom-up approach and combined scenario analyses to predict the future trend of China's carbon emissions in the building industry. The CBCEM model is based on the carbon emission formula (emission = activity level × activity factor) proposed by the United Nations Intergovernmental Panel on Climate Change (IPCC), and the calculation method was constructed as follows:

$$\text{building carbon emission} = \text{floor area} \times \text{carbon intensity}.$$

Each model has its own advantages, disadvantages, and suitability, and these depend on the specific circumstances. Top-down models are particularly valuable for macroeconomic analyses and comprehensive energy policy planning [11]. However, they often overlook the technical intricacies of energy production and energy consumption, posing a challenge in accurately capturing the shifting patterns of CE [12]. Representative models

include the following three types: the computable general equilibrium model (CGE) [13,14], the Groundings–Enterprises–Markets model (GEM) [15], and the log-mean Divisia index model (LMDI) [16,17]. Zhu et al. [18] employed the CGE model to assess the economic and environmental consequences of the following three energy-intensive sectors: cement, steel, and construction. They also investigated the influences of these sectors on the CEs associated with the construction industry. Their findings indicated that carbon reduction efforts in construction have primarily relied on the implementation of energy-saving technologies within the steel and cement sectors. Bottom-up models provide detailed descriptions of technologies and effectively capture the influences of technological advancements on energy systems. However, they require detailed data on energy technologies [19]. Representative models include the Market Allocation Model (MARKAL) [20,21], the Asian-Pacific Integrated Model (AIM) [22,23], and the Long-range Energy Alternatives Planning system (LEAP) model [24,25]. Mirjat et al. [26] utilized the LEAP model to create a model of Pakistan's electricity system from 2015 to 2050. The results of the model projected a demand forecast of 1706.3 TWh for the year 2050, representing an average annual growth rate of 8.35%, which indicated a significant increase of 19 times the base-year demand.

There are two main methods for achieving building CE predictions during the operational stage, including computer simulations and the regression linear model method. Simulation-based approaches were adopted earlier than regression models as energy simulation software played a key role in estimating building energy consumption (BEC). The energy simulation results were then converted into building CE based on emissions factors [27]. Peng [28] utilized Ecotect and building information modeling to compute the CE associated with the entire life cycle of a building. The findings indicated that the operational stage contributed 85.4% of the total CE, while the construction and demolition stages accounted for 12.6% and 2%, respectively. Yang et al. [29] employed building information modeling to evaluate the carbon footprints of residential buildings. The findings revealed that the operational phase contributed to 69% of the overall greenhouse gas emissions, whereas the production of building materials accounted for 24%. In addition, Wu et al. [30] employed DeST3.0 software to simulate the CE associated with the entire life cycles of buildings. However, it is important to note that the simulation method has proven to be time-consuming and challenging to modify in real time. Gardezi and Shafiq [31] utilized a linear regression model to forecast the carbon footprints of residential buildings located in tropical Malaysia. Prior research has demonstrated the efficacy of simulation methods in accurately predicting a building's CE during the operational stage.

1.2.2. The Influence of Urban Form on Building CEs

Urban forms are a key means for controlling building CEs [32]. To address the challenges posed by climate change and energy crises, researchers have begun to explore the relationship between urban forms and building CEs. Carpio et al. [33] quantified the relationship between urban forms, land use, cover changes, and CEs, and their results showed that vegetation removed due to urban expansion represented the potential to absorb 373,900 tons of CO_2 per year. Yuan et al. [34] quantified the relationship between the spatial forms of small cities and CE, and their research results showed that improving urban space compactness and reducing complexity and fragmentation had positive impacts on CE efficiency. Dong et al. [35] researched the influence of urban morphology on CE, taking Beijing as an example, and the findings from their study revealed that in the northern region of Beijing, factors such as adjacency ratios, meshedness levels, and widths had significant positive impacts on CO_2 emissions. Ou et al. [36] adopted panel data to analyze the effect of urban forms on CEs, and their research results showed that the irregularity of urban forms may also lead to more CEs, and the compact urban land development model was conducive to reducing CEs. Fang et al. [37] studied the effect of urban forms on CEs, and their research findings demonstrated that increased urban continuity had an inhibitory effect on CEs while increased urban shape complexity had a positive influence on CEs.

Deng et al. [38] adopted the ECOTECT and HTB2 tools to simulate heating for the BEC and CEs of residential blocks, and then they evaluated the relationship between the block form parameters and the CEs or heating for the BEC in the cold regions of China. However, their quantitative analysis results focused more on the impact of block forms on heating for the BEC. The summary results revealed that a majority of the existing studies examining the relationship between urban forms and building CEs have primarily concentrated on the urban scale. Research specifically investigating the influence of urban morphological parameters on building CE at the block scale has been limited in scope.

1.2.3. Research Gap

Previous research has confirmed the feasibility of using simulation methods to predict building CEs during the operational stage and to examine the influence of block morphological parameters on building CEs. However, the specific law of the combined impacts of block form parameters on building CEs has not been comprehensively analyzed. Such an understanding is crucial for future optimal design approaches in the low-carbon planning and design of residential blocks. It is imperative to enhance our understanding of the influences of block form parameters on building CEs. Notably, there is limited existing research that provides precise assessments of building CEs for residential blocks in China, particularly based on the climatic conditions in central China.

1.3. Research Objectives and Questions

In this work, our objectives were to assess the building carbon emissions intensity (CEI) during the operational phase of residential blocks using the Rhino and Grasshopper methods and to analyze the impact law of the block morphological parameters on the buildings' CEI. Specifically, this work's focus was on addressing the following three key questions:

- How much do the building CEI levels in different residential blocks vary?
- Which residential block form parameters have impacts on the buildings' CEI? Which ones do not matter? What is the most significant form parameter affecting the buildings' CEI?
- What are the combined parameters that most significantly affect the buildings' CEI?

2. Materials

2.1. The Framework

The overall technical workflow for this work was broken down into four steps, as shown in Figure 2. Step 1 involved case selection and block form parameters. Step 2 involved the calculation of CEs for block building complexes. Step 3 examined the relationship between block form parameters and buildings' CEI. Step 4 analyzed low-carbon planning strategies for urban blocks.

2.2. Case Selection and Classification

With the goal of analyzing the relationship between block forms and buildings' CEI, this study assumed that the block building envelope and the window-to-wall ratio had a fixed value that was determined through investigation. This study needed to ensure that the difference in the block scale and block building number in each case was not large. The case selection principle was that the land area of the residential block case was less than 1 km^2, and the number of buildings in the block had to be greater than 3 to form a group of buildings. For the case-based selection criteria, this paper selected 48 residential block cases in Wuhan from a satellite map and field investigations. Wuhan is representative of cities in China, with a climate that features hot summers and cold winters. The average yearly temperature in Wuhan ranges from 15.8 °C to 17.5 °C. During the summer season, in July, temperatures can reach a maximum of 37~39 °C and a minimum of 29~30 °C, resulting in a humid and uncomfortable environment. In January, the coldest month in winter, the

average temperature drops to 3.7 °C while the lowest temperatures range from −4.2 °C to −2.2 °C, creating a relatively cold and dreary atmosphere.

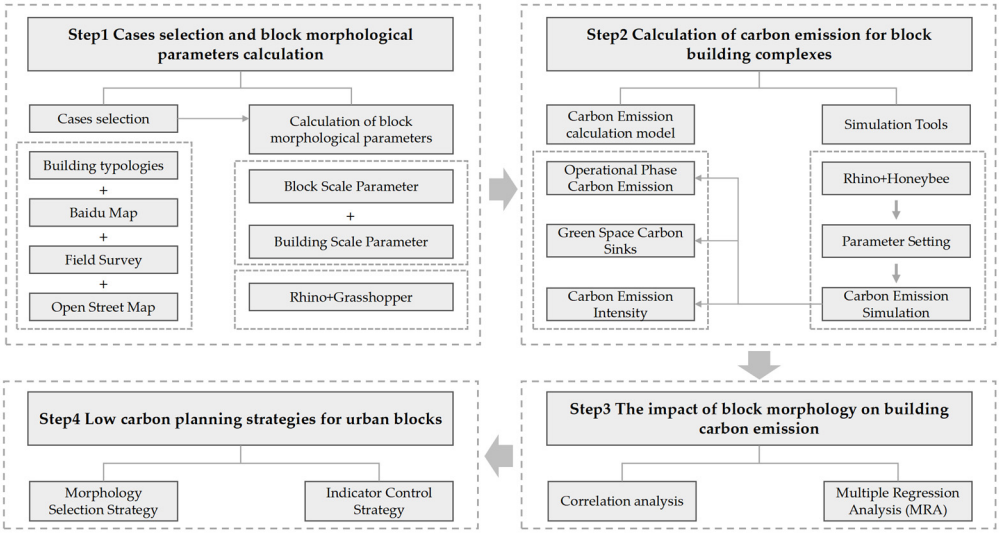

Figure 2. The overall technical workflow showing the four steps.

The architectural typology method has been extensively employed to investigate the influence of urban block form on environmental performance [39,40]. Combined with the research results and field survey results, this paper divided residential blocks into 3 categories and 8 subcategories according to the block plane shape and the block height change. They were, respectively, multi-story pavilion, multi-story slab, multi-story courtyard, mid-rise pavilion, mid-rise slab, mid-rise courtyard, high-rise pavilion, and high-rise slab. Table 1 shows the classification results for the block typologies.

2.3. Urban Block form Parameter Calculation

A block form is a material space form composed of urban buildings and their enclosed open spaces within a block area [41]. Urban block CEs are closely related to urban block form parameters, which has been proven by researchers [32,35]. Block form affects a building's CE and green space carbon sink by influencing the building energy demand [42,43] and the microclimate environment [44,45]. The research methods approach adopted in this work were intended to influence the building energy consumption (BEC) and carbon sink through block form and then affect the building CE. For residential blocks, form parameters can quantify the layout, building height, and construction intensity [39,46]. Combined with previous studies, this paper calculated some typical block form parameters to characterize the form features of residential blocks, such as height–depth ratio (H/D), length–depth ratio (L/D), building shape factor (BSF), orientation (O), building cover ratio (BCR), floor area ratio (FAR), sky view factor (SVF), building height (BH), building volume–site area ratio (V/S), building surface–site area ratio (S/A), and green space ratio (GSR). The definitions, calculation formulas, and schematic diagram of the form parameters are shown in Table 2. The process used to calculate the block morphological parameters is described below. Firstly, a combination of open street maps (OSM) and satellite maps was used to obtain a floor plan for each residential block. Secondly, the height and window-to-wall ratio information of each building in the residential block was obtained using a combination of field research and street maps. Thirdly, a 3D model of the residential block was built based on this geometric information. This method has been proven to be scientific and feasible by scholars [40]. The process of calculating the morphological parameters of a block is shown in Figure 3. The data characteristics of the block form parameters for the 48 selected cases are shown in Supplementary Materials.

Table 1. Classification results of 48 residential blocks.

Typologies	Building Height (m)	Block Case	Block 3D Model
Multi-story pavilion	H ≤ 27 m		
Multi-story slab	H ≤ 27 m		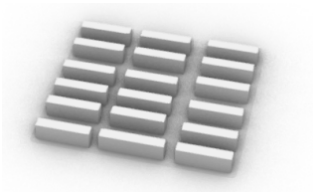
Multi-story courtyard	H ≤ 27 m		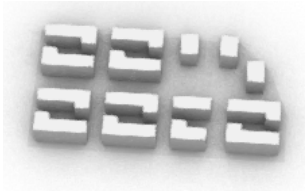
Mid-rise pavilion	27 < H ≤ 54 m		
Mid-rise slab	27 < H ≤ 54 m		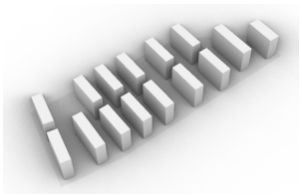
Mid-rise courtyard	27 < H ≤ 54 m		
High-rise pavilion	54 < H ≤ 99 m		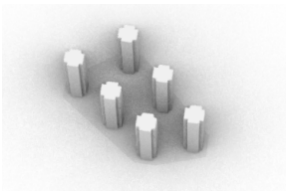
High-rise slab	54 < H ≤ 99 m		

Table 2. Definition and calculation formula of residential block morphological parameters.

Parameters	Formula	Definition	Diagram
H/D	$H/D = \frac{\sum_{i=1}^{n} h_i V_i}{\sum_{i=1}^{n} V_B} / \frac{\sum_{i=1}^{n} l_i V_i}{\sum_{i=1}^{n} V_B}$	h_i denoted building height of building i; V_i denoted building volume of building i; l_i denoted building length of building i; V_B denoted the total building volume	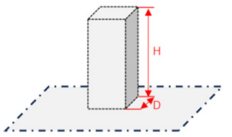
L/D	$L/D = \frac{\sum_{i=1}^{n} l_i V_i}{\sum_{i=1}^{n} V_B} / \frac{\sum_{i=1}^{n} D_i V_i}{\sum_{i=1}^{n} V_B}$	D_i represented building depth of building i	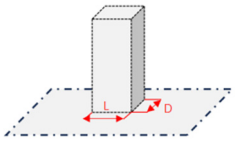
BSF	$BSF = \frac{S_B}{V_B}$	S_B represented the total building surface area	
O	$O = \frac{\sum_{i=1}^{n} O_i V_i}{\sum_{i=1}^{n} V_B}$	O_i represented the building orientation of building i	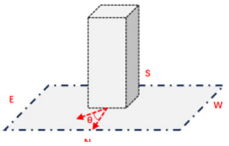
BCR	$BCR = \frac{S_D}{S_G} \times 100\%$	S_D denoted the total footprint area	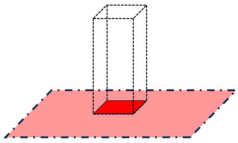
FAR	$FAR = \frac{S_F}{S_A}$	S_F denoted the total floor area; S_A represented the total site area	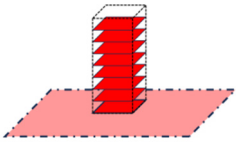
SVF	$SVF = \frac{R_P}{R_G}$	R_P was the solar radiation received from the visible sky at a point on the block; R_G was the global horizontal radiation received by the unobstructed hemisphere of the sky	
BH	$H/D = \frac{\sum_{i=1}^{n} h_i V_i}{\sum_{i=1}^{n} V_B}$	/	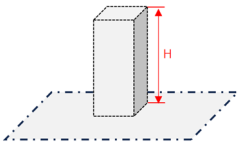
V/A	$V/A = \frac{V_B}{S_A}$	/	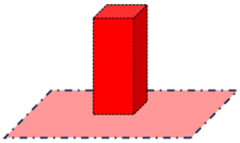

Table 2. *Cont.*

Parameters	Formula	Definition	Diagram
S/A	$S/A = \frac{S_B}{S_A}$	/	
GSR	$GSR = \frac{S_G}{S_A}$	S_G represented the green space area	

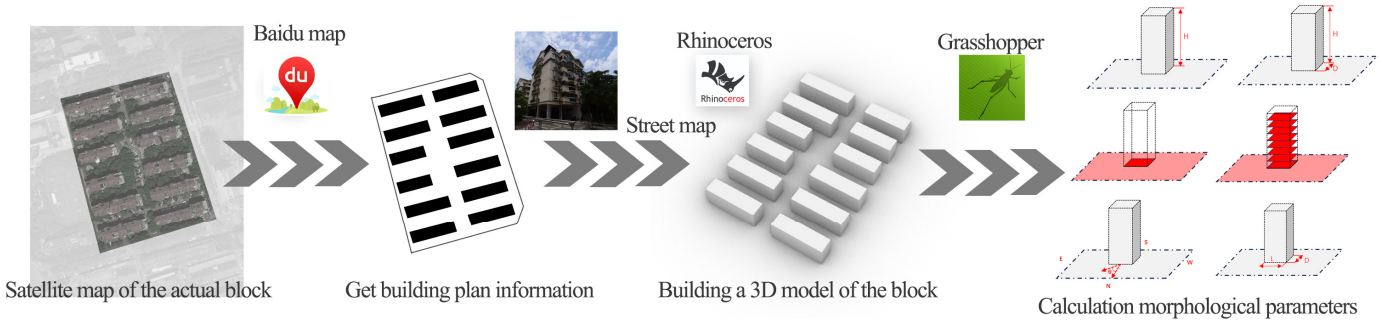

Figure 3. The process of calculating the morphological parameters of the block.

2.4. Building CE Calculation Method and Simulation Tool

2.4.1. Calculation Method for the Building CEs

To conduct a carbon emissions (CEs) assessment of residential blocks based on carbon emissions calculation standards [47], the calculation for a building's CE should be carried out according to the different requirements of each stage, and the results of the subsection calculation can be added to the building's CE for its whole life. In addition, the standard clearly states that a building's CE is calculated for either a single building or a complex. In this study, the building's CE was defined as its CE during the operational stages of residential block buildings. It included two aspects: (1) the CE of the buildings during their service lives; and (2) the carbon sinks of the green spaces during the buildings' service lives. Based on the survey results, there were fewer solar photovoltaic installations in residential blocks in Wuhan at this stage, and so the carbon reduction amounts for solar photovoltaics were not considered in this study.

Combined with relevant standards [47] and literature research [27,48], the building CE calculation model for the residential blocks was as follows:

$$C_M = \frac{(E_{ele}EF_{ele} - C_p) \times y}{A} \quad (1)$$

$$C_p = S_g \times \eta \times K_t \quad (2)$$

where C_M is the building CE per unit of building area during the operational stage (kg CO_2/m^2), E_{ele} is the whole-year building energy consumption (BEC) of the residential blocks (including the energy consumption for cooling, heating, lighting, and electrical equipment (kWh/y)), EF_{ele} is the electric power carbon emissions factor (which was 0.801 kg/kWh [49]), y is the service life period (y) (which was 50 [47]), A is the total floor area of the residential block (m^2), C_P is the annual carbon reduction in the building's green space carbon sink system (kg CO_2/y), S_g is the area of the green space carbon sink system

(m^2), η is the ratio of the tree cover (which was 30% [27]), and K_t is the carbon sink factor (kg $CO_2/m^2/y$) (which was 0.112 kg $CO_2/m^2/y$ [50]).

The calculation of the building CE of the residential blocks was carried out using a bottom-up method, and the annual BEC (electric power) of the buildings was simulated and calculated by energy consumption simulation software, employing Formula (1).

2.4.2. Building Carbon Emissions Simulation Tool

Relevant research on building energy consumption predictions [48] has shown that the mainstream hourly building energy consumption simulation software packages include DOE-2, eQUEST, ESR-r, and Energy Plus. Research on block-scale building energy consumption prediction [40,51] has shown that Energy Plus takes into account the impact of a building's surrounding environment on its BEC. This study considered the integration and operability of software platforms for 3D modeling and energy consumption simulation, and it adopted the Rhino and Grasshopper parametric platforms as simulation tools. The simulation tools used in this study have been validated in previous studies by our team [40,51]. This study employed the Ladybug Tools simulation plug-in to realize the residential block building energy consumption simulation, and the simulation process is shown in Figure 4.

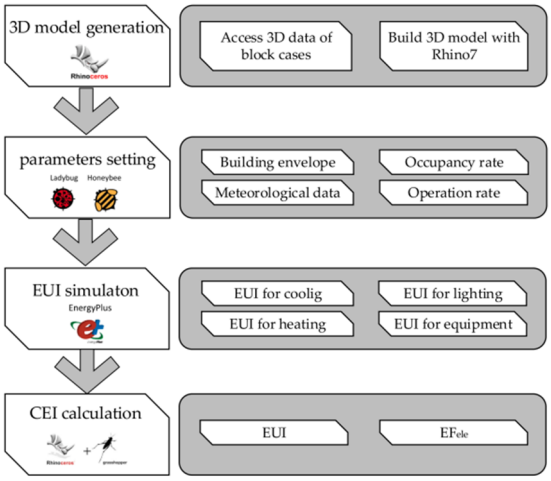

Figure 4. Building CE simulation based on Rhino and Grasshopper.

1 Simulation Parameter Setting

There are many factors that affect a building's CE during the operational stage. In the simulation calculation for the BEC throughout an entire year, the main research points in this work were the influence of the block form parameters on the building CE, and we set the building thermal parameters in combination with the relevant codes and standards [52] as well as energy saving reports from typical projects. The meteorological data parameters were set by using typical meteorological year files. The personnel activities and equipment operation parameters were set according to relevant standards. Tables 3 and 4 describe the specific settings of the simulation parameters.

2 Building carbon emissions (CE) calculation

Based on the Rhino and Grasshopper parametric platforms, the Energy Plus computing kernel was employed to simulate the annual building energy consumption (BEC) of the residential block. This study quantitatively analyzed the BEC by using the building energy consumption intensity (*EUI*). The building carbon emissions intensity (*CEI*) was used to quantify the building CE of the residential blocks, and its calculation formula is as follows:

$$EUI = \frac{E}{S_A} \quad (3)$$

$$CEI = EUI \times EF_{ele} \quad (4)$$

where *EUI* is the annual energy use intensity per unit of building area (kWh/m^2/y), *E* is the total annual BEC of the residential blocks (kWh/m^2/y), S_A is the total floor area of a residential block (m^2), and *CEI* is the annual building carbon emissions intensity per unit of building area (kg CO_2/m^2/y).

Table 3. Parameter setting for simulation.

	Parameter	Parameter Data	Source of Data
Climate Data	The Meteorological Data	Meteorological Data of Wuhan	China Meteorological Data Network
	Human Thermal Load	108 W/Person	JGJ/T449-2018
	Occupancy Rate	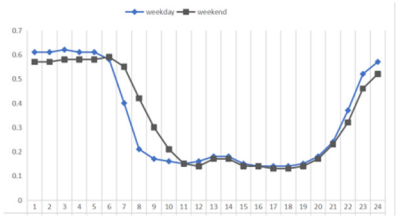	
Air Conditioning System	System Type	Split air conditioner for home use	Investigate and research
	Temperature Set	Cooling Set Point 26 °C Heating Set Point 18 °C	JGJ134-2010
	Operation Rate of Cooling	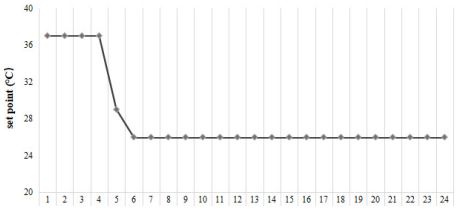	JGJ/T449-2018
	Operation Rate of Heating	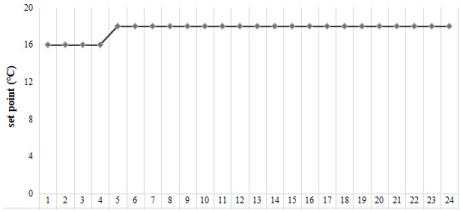	JGJ/T449-2018
Lighting	Power Density	3 W/m^2	Validation of experimental corrections
	Operation Rate of Lighting	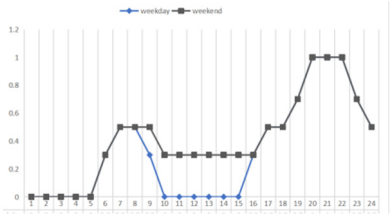	JGJ/T449-2018
Equipment	Power Density	4 W/m^2	Validation of experimental corrections
	Operation Rate of Equipment	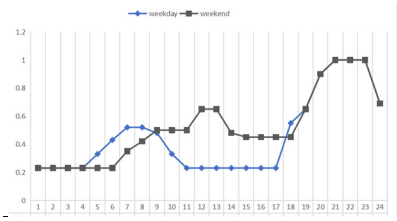	JGJ/T449-2018

Table 4. Parameter setting of building envelope.

Building Envelope		Heat Transfer Coefficient K (W/m^2·K)
Transparent envelope	Window	2.30
Opaque envelope	Roof	0.35
	Exterior wall	1.18
	Floor	1.14
	Interior wall	0.79

3. Results and Discussion

3.1. Building CE Distribution Characteristics of the Residential Blocks

3.1.1. Building CE Distribution Characteristics of All the Blocks

The distribution characteristics of the building CEIs for the service lives of the 48 residential blocks in Wuhan are shown in Figure 5. The data results demonstrated in the figure show that different residential blocks had different distributions of their building CEIs, and the building CEIs for the buildings' service lives ranged from 1070 to 1570 kg CO_2/m^2. Among these, the residential block with the smallest building CEI for its service life was A10, with 1073.08 kg CO_2/m^2, while the residential block with the largest building CEI for its service life was A3, with 1569.79 kg CO_2/m^2.

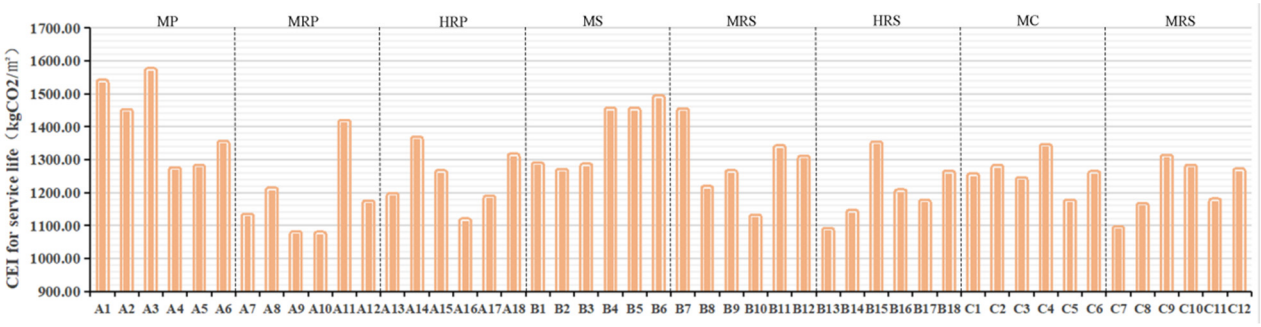

Figure 5. Distribution characteristics of the CEIs for the service lives of the 48 residential blocks.

The difference in the buildings' CEI caused by the block forms was 31.66%, which was slightly higher than the difference in the building energy consumption (BEC) in the operational stage caused by the block forms. The block form can have a significant impact, ranging from 10% to 30% or more, on the BEC [35,53]. In a study conducted by Xu et al. [40] in Wuhan, China, the impact of block forms on the BEC during the operational stages of office buildings was examined. Their research findings indicated a 13.88% difference in the BEC influenced by factors such as the BCR, FAR, and BSF. Similarly, Mangan et al. [54] assessed the influence of block form, such as the road height–width ratio, building typologies, and orientation, on the BECs of residential buildings during their operational stages. According to their research findings, increases in the heights of different building types, including the rectangular point type, rectangular panel type, and square enclosed type, resulted in reductions in their BECs by 14%, 8%, and 18%, respectively. For pavilion blocks, the fluctuation range in the building CEIs for their service lives was 1073.78–1569.79 kg CO_2/m^2. For slab blocks, the fluctuation range in the building CEIs for their service lives was 1084.76–1486.91 kg CO_2/m^2. For courtyard blocks, the fluctuation range in the building CEIs for their service lives was 1089.94–1339.14 kg CO_2/m^2.

The building CEIs of the 48 residential blocks in Wuhan are shown in Figure 6. The data results shown in the figure demonstrate that the building CEI in each block was different, and the building CEIs were between 21 and 32 kg $CO_2/m^2/y$. Among these, the residential block with the smallest building CEI was A10, with 21.46 kg $CO_2/m^2/y$, while the residential block with the largest building CEI was A3, with 31.40 kg $CO_2/m^2/y$. The average building CEI for all the blocks was 25.35 kg $CO_2/m^2/y$. This average building CEI value was higher than that of the urban buildings in the Greater Bay Area cities in

China during their operational stages, with 39.25 kg $CO_2/m^2/y$ [36]. A comparison of the building CEIs of the residential blocks during their operational stages in Wuhan City with those of previous studies [49,55,56] is shown in Figure 7.

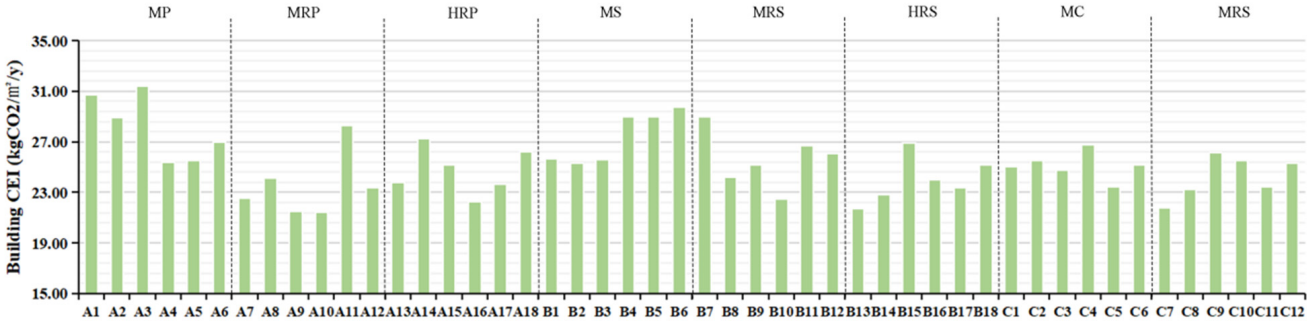

Figure 6. Distribution characteristics of the CEIs of the residential buildings for the 48 blocks.

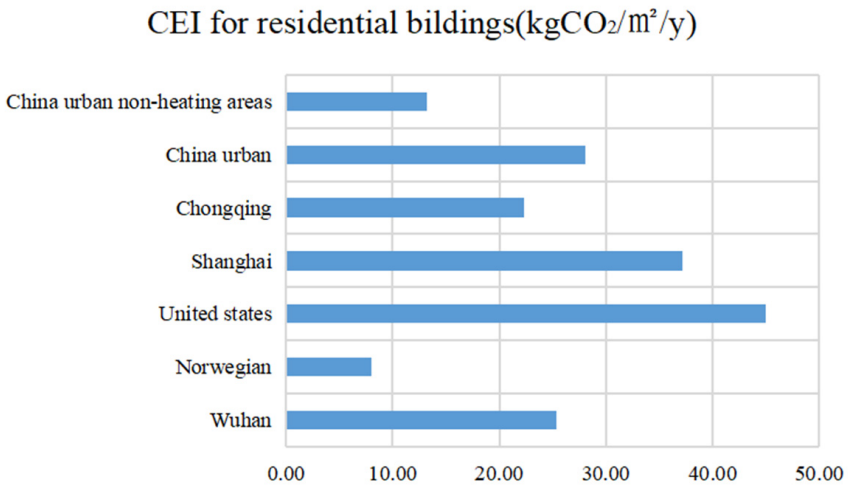

Figure 7. CEIs of residential buildings in different cities.

3.1.2. Building CE Distribution Characteristics for Different Block Typologies

The carbon emissions characteristics of different types of blocks are shown in Figure 6. For the data results described in Figure 8, in terms of the building CEI for the service life, the multi-story pavilion (1407.52 kg CO_2/m^2) and multi-story slab (1368.98 kg CO_2/m^2) typology values were higher than those of the mid-rise slab (1280.76 kg CO_2/m^2), multi-story courtyard (1255.77 kg CO_2/m^2), high-rise pavilion (1236.63 kg CO_2/m^2), and mid-rise courtyard (1212.09 kg CO_2/m^2), while the high-rise slab (1200.21 kg CO_2/m^2) and mid-rise pavilion (1177.38 kg CO_2/m^2) had lower building CEI values. For the data results shown in Figure 9, the building CEIs for each type of block showed the same trend, and their values were 28.16 kg CO_2/m^2y, 27.39 kg $CO_2/m^2/y$, 25.62 kg $CO_2/m^2/y$, 25.11 kg $CO_2/m^2/y$, 24.73 kg $CO_2/m^2/y$, 24.25 kg $CO_2/m^2/y$, 24.01 kg $CO_2/m^2/y$, and 23.55 kg $CO_2/m^2/y$, respectively.

3.2. The Relationship between Block Form and Building CE

3.2.1. Building CE Distributions for the Different Block Typologies

Using the calculated values of the form parameters in the residential blocks and the assessment results for the CEIs during operation, this section analyzed the impact of the residential blocks' morphological parameters on the buildings' CE. A building's CEI was considered as the building's carbon emissions and carbon sinks. This study took the building carbon emissions as the dependent variable Y and the residential block form parameters as the independent variable X, and it adopted the correlation analysis method to conduct a correlation analysis between the two variables. The scatter diagrams for the

residential blocks' form parameters and the buildings' CEIs are shown in Figure 10, and the correlation analysis results are shown in Figure 11 and Table 5. If the significance value (p) was below 0.05, it indicated a significant correlation between the independent variable and the dependent variable. The correlation analysis results showed that there was no correlation between the H/D, L/D, and GSR and a building's CEI. There was a negative correlation between the O, BCR, and S/A and a building's CEI, and there was a positive correlation between the SVF and a building's CEI, but it was not significant. Although there was a positive correlation between the SVF and a building's CEI, it was not found to be statistically significant. On the other hand, there was a significant positive correlation between the BSF and a building's CEI at the 0.01 level. Similarly, there was a significant negative correlation between the FAR and V/A and a building's CEI at the 0.01 level. Additionally, the BH demonstrated a significant negative correlation with a building's CEI at the 0.01 level. The BSF had the highest impact on a building's CEI, accounting for 0.910 of its correlation coefficient (r). This was followed by the FAR, with a correlation coefficient of -0.547, then the V/A, with a correlation coefficient of −0.547, and lastly, the BH, with a correlation coefficient of −0.328.

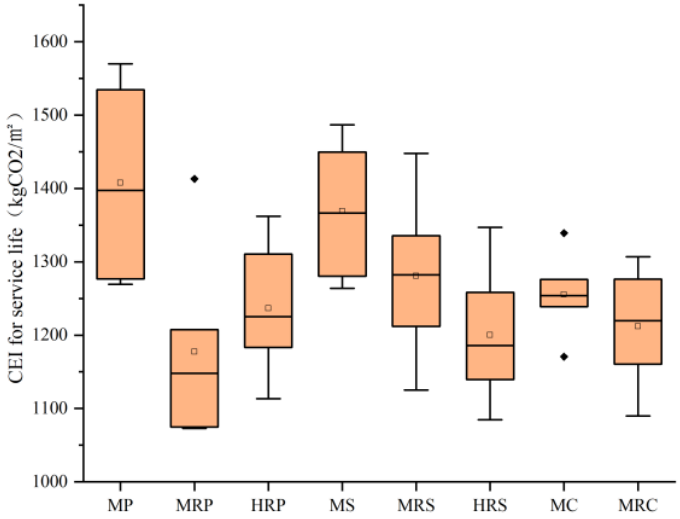

Figure 8. CE characteristics of the different block typologies for their service lives.

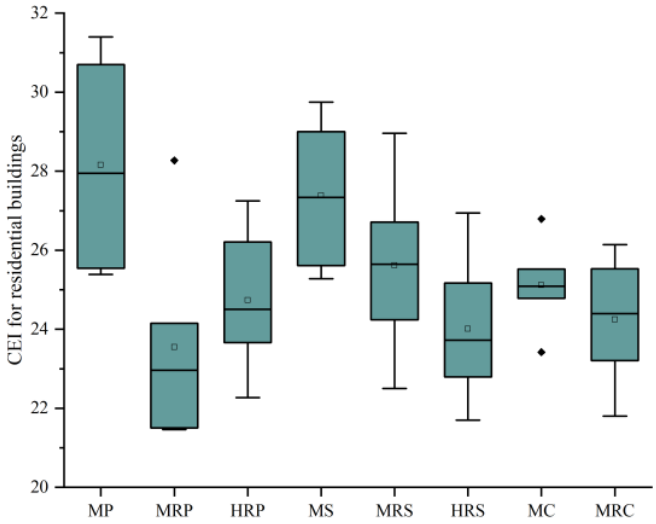

Figure 9. CE characteristics of the different block typologies.

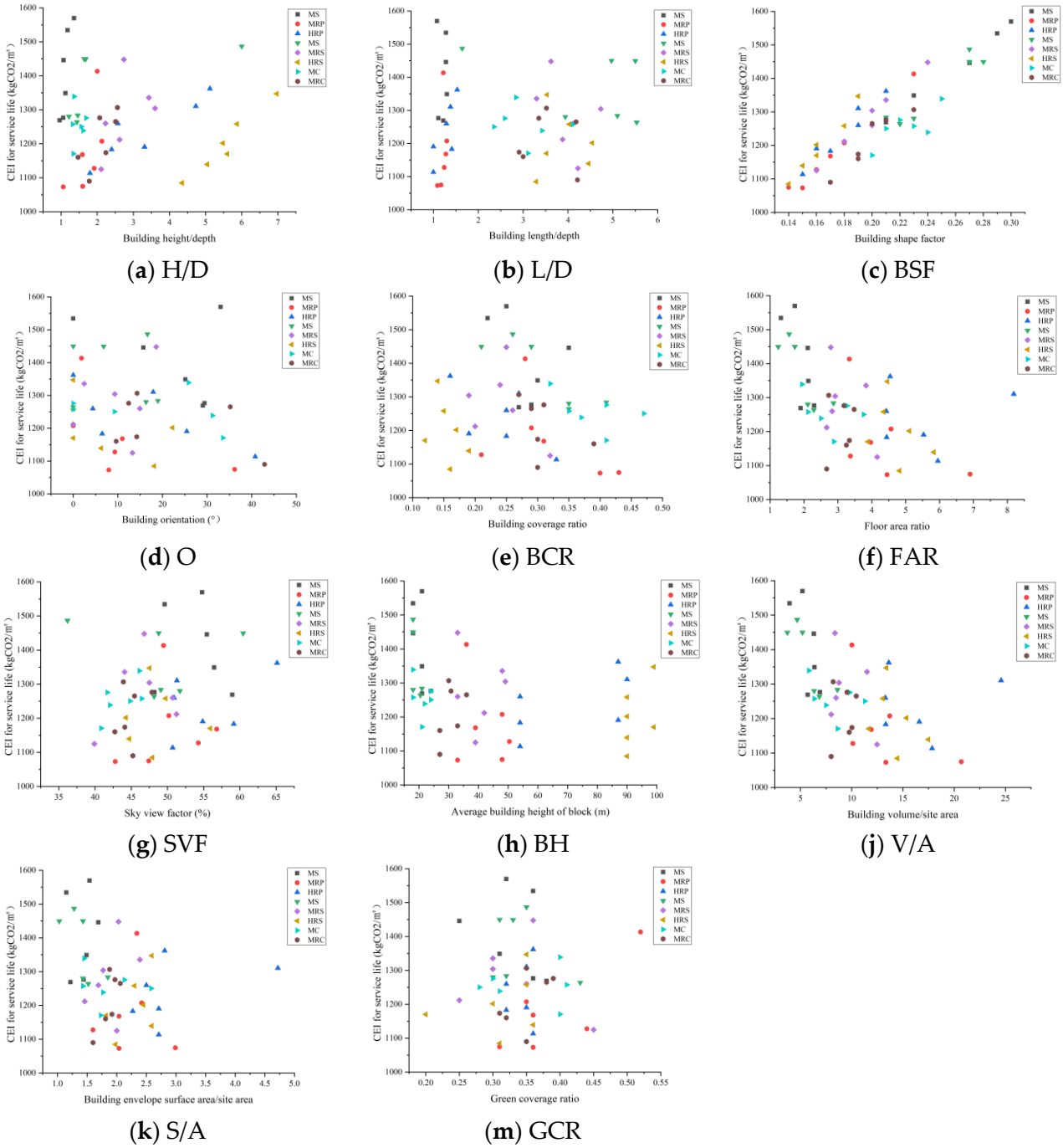

Figure 10. The scatter diagrams of morphological parameters and building CEI. The subfigure of (**a**–**m**) represent the scatter diagrams between H/D, L/D, BSF, O, BCR, FAR, SVF, BH, V/A, S/A and GCR and building CEI for service life, respectively.

Among the block form parameters related to a building's CEI, there was a positive correlation between the BSF and the CEI, indicating that the CEI advances with increases in the BSF. On the other hand, the BCR, FAR, BH, V/A, and CEI showed negative correlations, suggesting that a building's CEI decreases as these variables increase. Additionally, the magnitude of the correlation coefficient r indicated the strength of the relevance. Among these parameters, the BSF, FAR, BH, and BCR were considered representative form parameters. Taking Beijing as an example, Dong et al. [35] investigated the influence of building form and street form on a building's CE by using a geographically weighted regression method, and their research findings indicated a negative correlation between the BCR/FAR

and the CE. Their results supported the findings of this study. As the building shape factors of the blocks increased, so did the buildings' CE. This finding was consistent with those of previous studies, for example, studies in which the increases in block building shape factors increased the electricity energy consumption levels of urban residential blocks [57,58] and university campus dormitory blocks [54]. In addition, Xu et al. [40] used office blocks in Wuhan city as an example to study the effect of block form parameters on building energy consumption (BEC). Their research results showed that the BSF was positively correlated with the BEC while the BH, BCR, and FAR were negatively correlated with the BEC, which supported the research conclusions of this study.

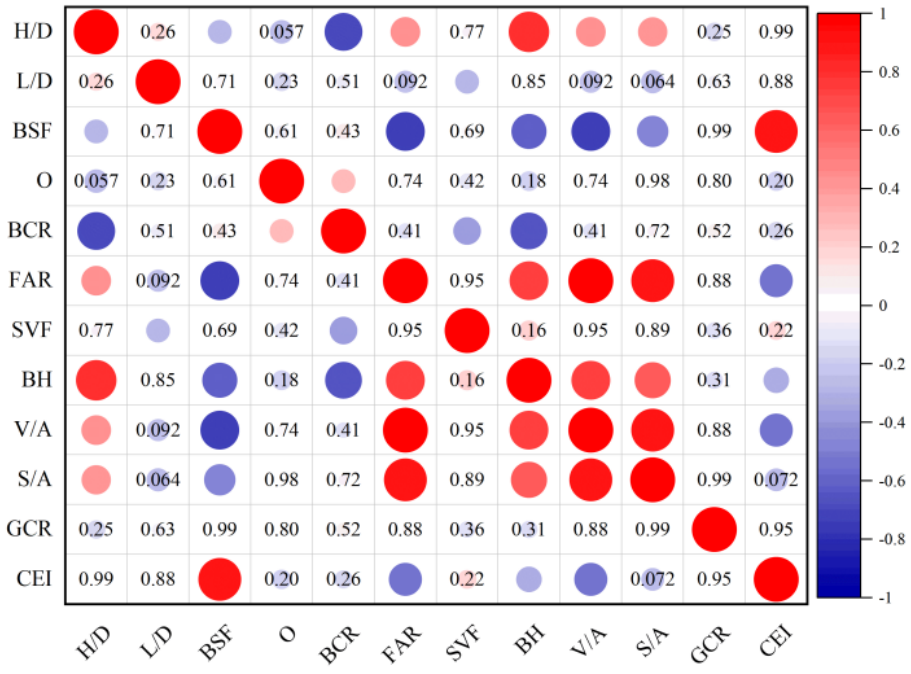

Figure 11. The correlations analysis results.

Table 5. The correlation analysis results.

	H/D	L/D	BSF	O	BCR	FAR
r	0.002	−0.023	0.910 **	−0.19	−0.164	−0.547 **
p	0.978	0.877	0.000	0.195	0.265	0.000
	SVF	BH	V/A	S/A	GCR	
r	0.181	−0.328 *	−0.547 **	−0.262	−0.005	
p	0.219	0.023	0.000	0.072	0.947	

*. means the correlation was significant at level of 0.05; **. means the correlation was significant at level of 0.01.

3.2.2. The Combined Impact of Block Form Parameters on a Building's CEI

Statistical analysis methods such as multiple linear regression models are widely used in the field of BEC and low carbon emissions [38,59]. The scatterplots and correlation analysis results of the block form parameters and the buildings' CEIs showed that a correlation was observed between the buildings' CEIs and multiple form parameters. Therefore, this study adopted a multiple linear regression analysis method to quantify the impact of the form parameters on a building's CEI. Before constructing the multiple linear regression equation, it was necessary to analyze the correlations and *p*-values among the form parameters of the residential blocks to determine whether there was multi-collinearity among the independent variables. The analysis results are shown in Figure 9. According to the data results in the figure, there was an auto-correlation between the BH and the H/D, FAR, S/A, and V/A.

After removing the auto-correlation variables, a multiple linear regression equation was constructed based on the SPSS25.0 software using a step-by-step method. The multiple linear regression coefficient and goodness of fit between the residential block form parameters and the buildings' CEIs are shown in Table 6. The multiple linear regression equation used for the buildings' CEIs and the block form parameters is as follows:

$$y = 641.271 + 3169.088x_1 + 46.056x_2 - 400.613x_3 \quad (5)$$

where y represents a building's CEI, x_1 denotes the BSF, x_2 represents the S/A, and x_3 denotes the BCR.

Table 6. The results for multi-linear regression model.

Dependent Variables	Independent Variables	Unstandardized Coefficients		Beta	t	*p*	VIF	R^2
		B	Standard Error					
CEI	(Constants)	641.271	37.671	-	17.023	0.000	-	0.944
	BSF	3169.088	122.897	1.057	25.789	0.000	1.323	
	S/A	46.056	7.930	0.237	5.808	0.000	1.309	
	BCR	−400.613	52.338	−0.275	−7.654	0.000	1.014	

The standardization coefficient could quantify the impacts of different unit independent variables on a building's carbon emissions. As can be seen from Table 6, the standardization coefficients of the BSF, S/A, and BCR were 1.057, 0.237, and −0.275, respectively. The influences of the BSF and BCR on a building's CEI were greater than that of the S/A. The influence weight of the BSF on a building's CEI was 3.84 times that of the BCR, which was 4.46 times that of the S/A. The value of the regression coefficient R^2 for this multivariate equation was 0.944. The closer R^2 is to 1, the better the goodness of fit of this equation [60]. This indicated that the BSF, S/A, and BCR could better predict the building CEIs of the residential blocks. Furthermore, a significance value (p) of 0.000 indicated that the multi-linear regression model exhibited high statistical significance and reliability.

3.3. Low-Carbon Planning Strategies for Residential Blocks under the Goal of Carbon Neutrality

Existing studies have shown that block form is an important means for regulating building carbon emissions [32,35,42]. Leng et al. [61] took office blocks in Harbin, China as an example, and they analyzed the influence of block form on the BEC for heating. Based on the influence law between the morphological parameters and the BEC, they established the urban block planning and design framework under the guidance of energy conservation. Xu et al. [40] quantified the synergistic impact of block morphological parameters on the BEC using office blocks in Wuhan, China as case studies, and they proposed planning and architectural design strategies for urban office blocks under the guidance of energy conservation. On the basis of the influence law of residential block form on building CE, this study put forward low-carbon planning strategies for residential blocks under the goal of carbon neutrality, including the following two aspects: block typology selection strategies and form index control strategies.

3.3.1. Block Typology Selection Strategies

According to the analysis results for the building CEIs of the different types of blocks, the mid-rise pavilion block A10 had the lowest building CEI, with 1073.08 kg CO_2/m^2. The multi-story pavilion block A3 had the highest building CEI, with 1569.79 kg CO_2/m^2. The distribution trend for the building CEIs of the eight typologies of residential blocks was MRP < HRS < MRC < HRP < MC < MRS < MS < MP.

Therefore, the low-carbon planning strategies for the block typology selection of residential blocks under the goal of carbon neutrality were as follows: for overall residential blocks, priority should be given to the construction of mid-rise pavilion blocks, high-rise

slab blocks, and mid-rise courtyard blocks. For the low-carbon planning and block typology selection of multi-story residential blocks, priority should be given to the construction of multi-story courtyards, multi-story slabs, and multi-story pavilions. For the low-carbon planning and block typology selection of mid-rise residential blocks, priority should be given to the construction of mid-rise pavilions, mid-rise slabs, and mind-rise courtyards. For high-rise residential blocks, priority should be given to the construction of high-rise slabs and high-rise pavilions.

3.3.2. Form Index Control Strategies

According to the multiple regression equation for building CEs and block form parameters, a building's CE was affected by the BSF, S/A, and BCR. The standardization coefficient Beta for the form parameters quantified the influence weight of the block form parameters on a building's CE, and we carried out normalization processing. The results showed that the standardized coefficients for the BSF, BCR, and FAR were 1.057, 0.237, and −0.275, respectively. Therefore, the form index control strategy for the low-carbon planning of residential blocks was to control the BAF, S/A, and BCR to achieve the lowest CE values for residential blocks within a reasonable range, and the morphological index control priority was the BSF, BCR, and S/A. The BSF and S/A should be controlled at a low level, and the BCR should be controlled at a high level. For every 0.1 unit increase in the BSF, the buildings' CEIs for the service lives of the residential blocks increased by 316.91 kg CO_2/m^2. Additionally, for each unit increase in the S/A, the buildings' CEIs of the residential blocks increased by 46.06 kg CO_2/m^2, while for every 10% increase in the BCR, the buildings' CEIs of the residential blocks were reduced by 40.06 kg CO_2/m^2.

3.4. Limitations and Future Research

Through our research hypothesis and control of the research variables, this work investigated the influence of block form parameters on building CE. In this paper, the parameters of the building envelopes, window–wall ratios, occupancy rates, and schedules were set as typical values. This paper did not take into account the difference in air-conditioning use schedules caused by the difference in economic and social characteristics of different households in the simulation process.

Future studies should aim to acquire more precise simulation parameters for each residential block, such as occupancy rates and building envelope data. In the simulation process, the relevant parameters for each building in the block were set separately so that the simulation results of the CE for the block buildings were closer to the real situations. This is very necessary to consider the difference of window wall ratio in different residential blocks, which can more finely simulate the influence of form parameters on building energy consumption, and it will be further expanded in the future work.

The methodology presented in this paper can be extended to other building types. When extending it to other building types, it should be noted that the building 3D model, meteorological parameters, thermal performance parameters, window-to-wall ratios, and other simulation parameters need to be adjusted before it can be applied.

This study was based on the assessment of the building CEs of residential blocks based on typical meteorological-year data. In order to realize the carbon peak of urban buildings in 2030 and carbon neutrality in 2060, future studies should consider conducting building carbon emissions assessments of residential blocks under future climate change conditions.

4. Conclusions

This study employed computer simulations to assess the building CEs of residential blocks in the hot summer and cold winter regions of China, using Wuhan as a case study. The impact of block form parameters on a building's CE was quantitatively analyzed. A statistical analysis method was used to identify the most influential parameters on a building's CE. The findings led to our proposal of low-carbon planning strategies for residential blocks. Some of our main findings are summarized as follows:

1. The results demonstrated that the block form influenced the building CEI by 31.66%.
2. The residential block with the smallest building CEI for its service life was A10, with 1073.08 kg CO_2/m^2. The residential block with the largest building CEI for its service life was A3, with 1569.79 kg CO_2/m^2.
3. The BSF had the greatest influence on a building's CEI, with r = 0.910, and this was followed by the FAR (r = −0.547), the V/A (r = −0.547), and the BH (r = −0.328).
4. The BSF, S/A, and BCR had a combined impact on a building's CEI. The influence weight of the BSF on a building's CEI was 3.84 times that of the BCR, which was 4.46 times that of the S/A.
5. For the low-carbon planning of residential blocks, a form index was the strategy used to control the BSF, S/A, and BCR to achieve the lowest building carbon emissions for residential blocks within a reasonable range, and the control priority of the form index was the BSF, BCR, and S/A.

The research findings presented in this paper can be utilized to assess block-scale building carbon emissions and provide low-carbon block planning strategies for urban designers, architects, and stakeholders. The technology workflow put forward in this study could provide data support for carbon emissions assessments and low-carbon planning strategies for urban blocks in other cities in China and worldwide.

Supplementary Materials: The following supporting information can be downloaded at: https://www.mdpi.com/article/10.3390/su152215751/s1.

Author Contributions: Conceptualization, H.L. and G.L.; methodology, G.L.; software, J.Z.; validation, H.L. and G.L.; formal analysis, G.L.; investigation, J.Z.; resources, H.L.; data curation, G.L.; writing—original draft preparation, H.L., G.L., R.R. and J.Z.; writing—review and editing, H.L., G.L. and R.R.; visualization, G.L.; supervision, G.L.; project administration, H.L.; funding acquisition, H.L. and G.L. All authors have read and agreed to the published version of the manuscript.

Funding: This research was funded by the Fundamental Research Funds for the Central Universities (YCJJ20230576), Cyrus Tang Foundation Inclusive Urban Planning and Research Scholarship (2022009), and Hebei Province Social Science Fund project (HB19YS039).

Data Availability Statement: The data presented in this study are available in Supplementary Materials.

Acknowledgments: The authors would like to thank all of the reviewers for their valuable contributions to this work.

Conflicts of Interest: The authors declare no conflict of interest.

Nomenclature

H/D	height–depth ratio of block
L/D	length–depth ratio of block
BSF	building shape factor
O	building orientation
BCR	building cover ratio
FAR	floor area ratio
SVF	sky view factor
BH	building height of block
V/S	building volume–site area ratio
S/A	building surface–site area ratio
GSR	green space ratio
CEI	building carbon emissions intensity
CE	carbon emissions
BEC	building energy consumption

References

1. Stocker, T. *Climate Change 2013: The Physical Science Basis: Working Group I Contribution to the Fifth Assessment Report of the Intergovernmental Panel on Climate Change*; Cambridge University Press: Cambridge, UK, 2014.
2. International Energy Agency (IEA). *Cities, Towns and Renewable Energy: Yes in My Front Yard*; OECD Publishing: Paris, France, 2009.
3. Dhakal, S. Urban Energy Use and Carbon Emissions from Cities in China and Policy Implications. *Energy Policy* **2009**, *37*, 4208–4219. [CrossRef]
4. China Association of Building Energy Efficiency. *China Building Energy Consumption Research Report 2020*; China Association of Building Energy Efficiency: Shanghai, China, 2020.
5. Central People's Government of the People's Republic of China. Actively and Steadily Promoting Carbon Peaking and Carbon Neutrality. 2023. Available online: https://www.gov.cn/yaowen/2023-04/06/content_5750183.htm (accessed on 6 October 2023).
6. Qudong China. What We Have Done to Prepare for the "Dual-Carbon" Goal. 2021. Available online: https://www.qudong.com/article/783763.shtml (accessed on 6 October 2023).
7. Li, Z.; Lin, B.; Zheng, S.; Liu, Y.; Wang, Z.; Dai, J. A Review of Operational Energy Consumption Calculation Method for Urban Buildings. In *Building Simulation*; Springer: Berlin/Heidelberg, Germany, 2020; Volume 13, pp. 739–751.
8. Kavgic, M.; Mavrogianni, A.; Mumovic, D.; Summerfield, A.; Stevanovic, Z.; Djurovic-Petrovic, M. A review of bottom-up building stock models for energy consumption in the residential sector. *Build. Environ.* **2021**, *45*, 1683–1697. [CrossRef]
9. Yang, Y.; Li, H.; Zheng, H. Research on Factors of Beijing's Building Carbon Emissions. *Ecol. Econ.* **2016**, *32*, 72–75.
10. Yang, T.; Pan, Y.; Yang, Y.; Lin, M.; Qin, B.; Xu, P.; Huang, Z. CO2 emissions in China's building sector through 2050: A scenario analysis based on a bottom-up model. *Energy* **2017**, *128*, 208–223. [CrossRef]
11. Huo, T.; Xu, L.; Feng, W.; Cai, W.; Liu, B. Dynamic Scenario Simulations of Carbon Emission Peak in China's City-Scale Urban Residential Building Sector through 2050. *Energy Policy* **2021**, *159*, 112612. [CrossRef]
12. Böhringer, C.; Rutherford, T.F. Integrated Assessment of Energy Policies: Decomposing Top-down and Bottom-Up. *J. Econ. Dyn. Control* **2009**, *33*, 1648–1661. [CrossRef]
13. Hübler, M.; Löschel, A. The EU Decarbonisation Roadmap 2050—What Way to Walk? *Energy Policy* **2013**, *55*, 190–207. [CrossRef]
14. Thepkhun, P.; Limmeechokchai, B.; Fujimori, S.; Masui, T.; Shrestha, R.M. Thailand's Low-Carbon Scenario 2050: The AIM/CGE Analyses of CO_2 Mitigation Measures. *Energy Policy* **2013**, *62*, 561–572. [CrossRef]
15. Ciscar, J.-C.; Saveyn, B.; Soria, A.; Szabo, L.; Van Regemorter, D.; Van Ierland, T. A Comparability Analysis of Global Burden Sharing GHG Reduction Scenarios. *Energy Policy* **2013**, *55*, 73–81. [CrossRef]
16. Tan, X.; Dong, L.; Chen, D.; Gu, B.; Zeng, Y. China's Regional CO_2 Emissions Reduction Potential: A Study of Chongqing City. *Appl. Energy* **2016**, *162*, 1345–1354. [CrossRef]
17. Kang, J.; Zhao, T.; Liu, N.; Zhang, X.; Xu, X.; Lin, T. A Multi-Sectoral Decomposition Analysis of City-Level Greenhouse Gas Emissions: Case Study of Tianjin, China. *Energy* **2014**, *68*, 562–571. [CrossRef]
18. Zhu, W.; Huang, B.; Zhao, J.; Chen, X.; Sun, C. Impacts on the Embodied Carbon Emissions in China's Building Sector and Its Related Energy-Intensive Industries from Energy-Saving Technologies Perspective: A Dynamic CGE Analysis. *Energy Build.* **2023**, *287*, 112926. [CrossRef]
19. Yang, D.; Liu, D.; Huang, A.; Lin, J.; Xu, L. Critical Transformation Pathways and Socio-Environmental Benefits of Energy Substitution Using a LEAP Scenario Modeling. *Renew. Sustain. Energy Rev.* **2021**, *135*, 110116. [CrossRef]
20. Tsai, M.-S.; Chang, S.-L. Taiwan's 2050 Low Carbon Development Roadmap: An Evaluation with the MARKAL Model. *Renew. Sustain. Energy Rev.* **2015**, *49*, 178–191. [CrossRef]
21. Chiodi, A.; Gargiulo, M.; Rogan, F.; Deane, J.P.; Lavigne, D.; Rout, U.K.; Gallachóir, B.P.Ó. Modelling the Impacts of Challenging 2050 European Climate Mitigation Targets on Ireland's Energy System. *Energy Policy* **2013**, *53*, 169–189. [CrossRef]
22. Wen, Z.; Meng, F.; Chen, M. Estimates of the Potential for Energy Conservation and CO_2 Emissions Mitigation Based on Asian-Pacific Integrated Model (AIM): The Case of the Iron and Steel Industry in China. *J. Clean. Prod.* **2014**, *65*, 120–130. [CrossRef]
23. Su, X.; Zhou, W.; Sun, F.; Nakagami, K. Possible Pathways for Dealing with Japan's Post-Fukushima Challenge and Achieving CO_2 Emission Reduction Targets in 2030. *Energy* **2014**, *66*, 90–97. [CrossRef]
24. Chen, R.; Rao, Z.H.; Liu, J.X.; Chen, Y.Y.; Liao, S.M. Prediction of energy demand and policy analysis of Changsha based on LEAP Model. *Resour. Sci.* **2017**, *39*, 482–489. [CrossRef]
25. Nieves, J.A.; Aristizábal, A.J.; Dyner, I.; Báez, O.; Ospina, D.H. Energy Demand and Greenhouse Gas Emissions Analysis in Colombia: A LEAP Model Application. *Energy* **2019**, *169*, 380–397. [CrossRef]
26. Mirjat, N.H.; Uqaili, M.A.; Harijan, K.; Walasai, G.D.; Mondal, M.A.H.; Sahin, H. Long-Term Electricity Demand Forecast and Supply Side Scenarios for Pakistan (2015–2050): A LEAP Model Application for Policy Analysis. *Energy* **2018**, *165*, 512–526. [CrossRef]
27. Ye, Z.D.; Wang, J.Y. *Carbon Accounting for Chinese Cities Green District Plans: Methodology, Data and Evaluation Guidelines*; China Architecture & Building Press: Beijing, China, 2015.
28. Peng, C. Calculation of a Building's Life Cycle Carbon Emissions Based on Ecotect and Building Information Modeling. *J. Clean. Prod.* **2016**, *112*, 453–465. [CrossRef]

29. Yang, X.; Hu, M.; Wu, J.; Zhao, B. Building-Information-Modeling Enabled Life Cycle Assessment, a Case Study on Carbon Footprint Accounting for a Residential Building in China. *J. Clean. Prod.* **2018**, *183*, 729–743. [CrossRef]
30. Wu, X.; Peng, B.; Lin, B. A Dynamic Life Cycle Carbon Emission Assessment on Green and Non-Green Buildings in China. *Energy Build.* **2017**, *149*, 272–281. [CrossRef]
31. Gardezi, S.S.S.; Shafiq, N. Operational Carbon Footprint Prediction Model for Conventional Tropical Housing: A Malaysian Prospective. *Int. J. Environ. Sci. Technol.* **2019**, *16*, 7817–7826. [CrossRef]
32. Zhang, X.; Yan, F.; Liu, H.; Qiao, Z. Towards Low Carbon Cities: A Machine Learning Method for Predicting Urban Blocks Carbon Emissions (UBCE) Based on Built Environment Factors (BEF) in Changxing City, China. *Sustain. Cities Soc.* **2021**, *69*, 102875. [CrossRef]
33. Carpio, A.; Ponce-Lopez, R.; Lozano-García, D.F. Urban Form, Land Use, and Cover Change and Their Impact on Carbon Emissions in the Monterrey Metropolitan Area, Mexico. *Urban Clim.* **2021**, *39*, 100947. [CrossRef]
34. Yuan, Q.; Guo, R.; Leng, H.; Song, S. Research on the Impact of Urban Form of Small and Medium-Sized Cities on Carbon Emission Efficiency in the Yangtze River Delta. *J. Hum. Settl. West China* **2021**, *36*, 8–15.
35. Dong, Q.; Huang, Z.; Zhou, X.; Guo, Y.; Scheuer, B.; Liu, Y. How Building and Street Morphology Affect CO_2 Emissions: Evidence from a Spatially Varying Relationship Analysis in Beijing. *Build. Environ.* **2023**, *236*, 110258. [CrossRef]
36. Ou, J.; Liu, X.; Li, X.; Chen, Y. Quantifying the Relationship between Urban Forms and Carbon Emissions Using Panel Data Analysis. *Landsc. Ecol.* **2013**, *28*, 1889–1907. [CrossRef]
37. Fang, C.; Wang, S.; Li, G. Changing Urban Forms and Carbon Dioxide Emissions in China: A Case Study of 30 Provincial Capital Cities. *Appl. Energy* **2015**, *158*, 519–531. [CrossRef]
38. Deng, Q.; Wang, G.; Wang, Y.; Zhou, H.; Ma, L. A Quantitative Analysis of the Impact of Residential Cluster Layout on Building Heating Energy Consumption in Cold IIB Regions of China. *Energy Build.* **2021**, *253*, 111515. [CrossRef]
39. Tian, J.; Xu, S. A Morphology-Based Evaluation on Block-Scale Solar Potential for Residential Area in Central China. *Sol. Energy* **2021**, *221*, 332–347. [CrossRef]
40. Xu, S.; Li, G.; Zhang, H.; Xie, M.; Mendis, T.; Du, H. Effect of Block Morphology on Building Energy Consumption of Office Blocks: A Case of Wuhan, China. *Buildings* **2023**, *13*, 768. [CrossRef]
41. Urquizo, J.; Calderón, C.; James, P. Understanding the Complexities of Domestic Energy Reductions in Cities: Integrating Data Sets Generally Available in the United Kingdom's Local Authorities. *Cities* **2018**, *74*, 292–309. [CrossRef]
42. Leng, H.; Chen, X.; Ma, Y.; Wong, N.H.; Ming, T. Urban Morphology and Building Heating Energy Consumption: Evidence from Harbin, a Severe Cold Region City. *Energy Build.* **2020**, *224*, 110143. [CrossRef]
43. Filogamo, L.; Peri, G.; Rizzo, G.; Giaccone, A. On the Classification of Large Residential Buildings Stocks by Sample Typologies for Energy Planning Purposes. *Appl. Energy* **2014**, *135*, 825–835. [CrossRef]
44. He, B.-J.; Ding, L.; Prasad, D. Enhancing Urban Ventilation Performance through the Development of Precinct Ventilation Zones: A Case Study Based on the Greater Sydney, Australia. *Sustain. Cities Soc.* **2019**, *47*, 101472. [CrossRef]
45. Shashua-Bar, L.; Tsiros, I.X.; Hoffman, M.E. A Modeling Study for Evaluating Passive Cooling Scenarios in Urban Streets with Trees. Case Study: Athens, Greece. *Build. Environ.* **2010**, *45*, 2798–2807. [CrossRef]
46. Liu, K.; Xu, X.; Zhang, R.; Kong, L.; Wang, W.; Deng, W. Impact of Urban Form on Building Energy Consumption and Solar Energy Potential: A Case Study of Residential Blocks in Jianhu, China. *Energy Build.* **2023**, *280*, 112727. [CrossRef]
47. *GBT 51366-2019*; Ministry of Housing and Urban-Rural Development, PRC. Standard for Calculation of Building Carbon Emissions. China Architecture & Building Press: Beijing, China, 2019.
48. Pan, Y.Q.; Liang, Y.M.; Zhu, M.Y. Review of Building Carbon Emission Calculation Models in Context of Carbon Neutrality. *Heat. Vent. Air Cond.* **2021**, *51*, 37–48.
49. National Development and Reform Commission. *Guidelines for the Preparation of Provincial GHG Inventories (for Trial Implementation)*; National Development and Reform Commission, PRC: Beijing, China, 2011.
50. Wang, D.S. Studies on Net Carbon Reserves in Beijing Urban Landscape Green Based on Biomass Measurement. PhD Thesis, Beijing Forestry University, Beijing, China, 2010.
51. Xu, S.; Sang, M.; Xie, M.; Xiong, F.; Mendis, T.; Xiang, X. Influence of Urban Morphological Factors on Building Energy Consumption Combined with Photovoltaic Potential: A Case Study of Residential Blocks in Central China. *Build. Simul.* **2023**, *16*, 1777–1792. [CrossRef]
52. *DB 42/T559-2013*; Wuhan Building Energy Efficiency Office, Hubei Province Construction Technology Development Center Design Standard for Energy Efficiency of Residential Buildings. Chinese Building Materials Press: Beijing, China, 2013.
53. Strømann-Andersen, J.; Sattrup, P.A. The urban canyon and building energy use: Urban density versus daylight and passive solar gains. *Energy Build.* **2011**, *43*, 2011–2020. [CrossRef]
54. Xie, M.; Wang, M.; Zhong, H.; Li, X.; Li, B.; Mendis, T.; Xu, S. The Impact of Urban Morphology on the Building Energy Consumption and Solar Energy Generation Potential of University Dormitory Blocks. *Sustain. Cities Soc.* **2023**, *96*, 104644. [CrossRef]
55. Sandberg, N.H.; Bergsdal, H.; Brattebø, H. Historical Energy Analysis of the Norwegian Dwelling Stock. *Build. Res. Inf.* **2011**, *39*, 1–15. [CrossRef]
56. Goldstein, B.; Gounaridis, D.; Newell, J.P. The Carbon Footprint of Household Energy Use in the United States. *Proc. Natl. Acad. Sci. USA* **2020**, *117*, 19122–19130. [CrossRef]

57. Mousavi Sarvine Baghi, E.S.; Ranjbar, E. Seeking Low Carbon Urban Design through Modelling of Carbon Emission from Different Sources in Urban Neighbourhoods, Case Study: Semnan. *Int. J. Urban Sustain. Dev.* **2021**, *13*, 546–568. [CrossRef]
58. He, P.; Xue, J.; Shen, G.Q.; Ni, M.; Wang, S.; Wang, H.; Huang, L. The Impact of Neighborhood Layout Heterogeneity on Carbon Emissions in High-Density Urban Areas: A Case Study of New Development Areas in Hong Kong. *Energy Build.* **2023**, *287*, 113002. [CrossRef]
59. Tso, G.K.; Guan, J. A Multilevel Regression Approach to Understand Effects of Environment Indicators and Household Features on Residential Energy Consumption. *Energy* **2014**, *66*, 722–731. [CrossRef]
60. Fumo, N.; Biswas, M.R. Regression Analysis for Prediction of Residential Energy Consumption. *Renew. Sustain. Energy Rev.* **2015**, *47*, 332–343. [CrossRef]
61. Song, S.; Leng, H.; Guo, R. Planning Strategy for Urban Building Energy Conservation Supported by Agent-Based Modeling. *Buildings* **2022**, *12*, 2171. [CrossRef]